Commun. Comput. Phys.
doi: 10.4208/cicp.181209.040111s

Vol. **11**, No. 2, pp. 508-524
February 2012

A Low Frequency Model for Acoustic Propagation in a 2D Flow Duct: Numerical Computation

Lauris Joubert[1,*] and Patrick Joly[2]

[1] *POEMS, CNRS-INRIA-ENSTA UMR 2706, 32 Boulevard Victor, 75015 Paris, France.*
[2] *POEMS, CNRS-INRIA-ENSTA UMR 2706, INRIA Rocquencourt, BP 105, 78153 Le Chesnay Cedex, France.*

Received 18 December 2009; Accepted (in revised version) 4 January 2011

Available online 24 October 2011

Abstract. In this paper we study a low frequency model for acoustic propagation in a 2D flow duct. For some Mach profile flow, we are able to give a well-posedness theorem. Its proof relies on a quasi-explicit expression of the solution which provides us an efficient numerical method. We give and comment numerical results for particular linear, tangent and quadratic profiles. Finally, we give a numerical validation of our asymptotic model.

AMS subject classifications: 35B35, 35Q35, 35C15

Key words: Acoustics in flow, Galbrun's equations, asymptotic analysis, Laplace transform.

1 Introduction

The present work has been motivated by applications to computational aeroacoustics, namely the numerical modelling of the propagation of sound in a moving fluid. In this perspective, we have chosen to reconsider the problem from a fundamental point of view and to begin with the propagation of sound in a duct. We consider a strongly varying parallel flow which can be simply described with the help of a scalar function $M(y)$ which represents, after appropriate normalisation (it is the Mach number), the lateral variations of the velocity of the reference flow. We shall call this function the Mach profile. For this model problem, a quasi-1D mathematical problem has been obtained in [1] from Galbrun's equations [5] (which are equivalent to the well-known linearized Euler equations) by a formal asymptotic expansion with respect to the width of the tube (this can also be

*Corresponding author. *Email addresses:* lauris.joubert@gmail.com (L. Joubert), Patrick.Joly@inria.fr (P. Joly)

seen as a low frequency analysis). This model leads to the following initial value problem, where the unknown u is the limit (as the width tends to 0) of the x component of the Lagrange displacement:

$$\begin{cases} \text{Find } u(x,y,t): \mathbb{R}\times[-1,1]\times\mathbb{R}^+\to\mathbb{R}, \\ \left(\dfrac{\partial}{\partial t}+M(y)\dfrac{\partial}{\partial x}\right)^2 u-\dfrac{\partial^2}{\partial x^2}Eu=0, \quad (x,y)\in\mathbb{R}\times[-1,1], \quad t>0, \\ u(x,y,0)=u_0(x,y), \quad (x,y)\in\mathbb{R}\times[-1,1], \\ \dfrac{\partial u}{\partial t}(x,y,0)=u_1(x,y), \quad (x,y)\in\mathbb{R}\times[-1,1], \end{cases} \tag{1.1}$$

where $M\in L^\infty(]-1,1[)$ is the Mach profile and E is the following averaging operator on $L^2(]-1,1[)$:

$$E: u\to Eu=\frac{1}{2}\int_{-1}^{1}u(y)\,dy. \tag{1.2}$$

This model is local (differential) in x, the coordinate along the axis of the tube, but non local in y, the transversal coordinate. The paper [2] is devoted to the mathematical analysis of this problem, using the Fourier transform and spectral theory. Despite its apparent simplicity this problem has rather surprising properties. In particular, we exhibit in [2] a necessary condition for the problem to be well-posed and it was conjectured that it is a sufficient condition. The authors of [6] are able to show this conjecture for a class of smooth monotonous and convex (or concave) profiles. This was done by calculating a quasi-explicit expression of the solution, using the Fourier-Laplace transform. This present paper is devoted to the numerical computation of the solution of (1.1), hence it is based on the two articles [2] and [6]. In Section 2, after reminding some properties of (1.1), we give a new well-posedness theorem (2.1) based on the method used in [6]. Then we apply this theorem to the case of a class of smooth monotonous profiles for which more calculations can be done, to get Theorem 2.2. After that, the case of the quadratic profile $M(y)=1-y^2$ is explored, it constitutes an example of extension to non monotonous profiles. The proof of Theorem 2.1 relies on a quasi-explicit representation of the solution which is given; this representation of the solution will provide an efficient way to compute the solution. The numerical method is presented in Section 3 and is then illustrated, for smooth monotonous profiles, by the linear and tangent profiles, and for a non monotonous profile, by the quadratic profile $M(y)=1-y^2$. In the last section, we give a numerical validation of our asymptotic model by comparison to a 2D Eulerian code.

At this stage of the work, our contribution remains quite academic and several steps need to be done before asserting that this kind of approximate model is useful for the applications.

- Because of its non-local nature, our model is not easily tractable from the numerical point of view. However approximating the reference profile $M(y)$ by a piecewise

linear profile leads to a new model that is local: it couples a 1D PDE with ordinary differential equations in time. The derivation and the implementation of this model is currently under consideration.

- The 3D case (a thin 3D domain delimited by two parallel surfaces) is of course of fundamental interest. The quasi 2D limit model has already been derived in the case of plane surfaces (under natural assumptions on the reference flow). The general case requires further investigation involving differential geometry.
- An attractive application of this kind of model consists in deriving approximate boundary conditions for dealing with thin boundary layers of the reference flow (see for instance [3] for a general exposition of the problematic). This research is under way and preliminary results show that our approximate model is one of the ingredients in the equivalent boundary condition.

2 Well-posedness results and a quasi-explicit representation of the solution

Despite its apparent simplicity, the study of the well-posedness of (1.1) is a difficult problem (see [2] and [6]). We are here going to recall, quickly, the method and some of the results obtained in [6]. More precisely, we give a well-posedness theorem obtained for a class of smooth monotonous profiles. But first, we give a more general but less explicit theorem, for which the hypotheses will be, roughly speaking: "we can do the same calculation as in [6]". In both cases, we will give a quasi-explicit expression of the solution which will provide us an efficient method to compute numerically the solution.

2.1 Preliminary statements and results

From now on, we assume that $M\in C^0([-1,1])$ and we denote:

$$M_+ := \sup_{y\in[-1,1]} M(y), \qquad M_- := \inf_{y\in[-1,1]} M(y).$$

It is clear that, if Eu is known, (1.1) is a simple transport square equation along x, for each fixed y. We solve this transport equation explicitly:

$$\begin{aligned} u(x,y,t) =& u_0\big(x-M(y)t,y\big)+t\left[u_1\big(x-M(y)t,y\big)+M(y)\frac{\partial u_0}{\partial x}\big(x-M(y)t,y\big)\right] \\ &+\int_0^t (t-s)\frac{\partial^2}{\partial x^2}Eu\big(x-M(y)(t-s),s\big)\,ds. \end{aligned} \tag{2.1}$$

The idea followed in [6] is to calculate Eu by using the Fourier transform in x and the Laplace transform in t. We define the Fourier transform as an unitary operator on $L^2(\mathbb{R})$,

defined for $f \in L^1(\mathbb{R})$ as

$$(\mathcal{F}f)(k) = \hat{f}(k) := \frac{1}{\sqrt{2\pi}} \int_{-\infty}^{\infty} e^{-ikx} f(x)\, dx.$$

We denote by $\tilde{u}$ the Laplace transform in time of $\hat{u}$,

$$\tilde{u}(k,y,\omega) := \int_0^{\infty} e^{i\omega t} \hat{u}(k,y,t)\, dt, \qquad \mathcal{I}m(\omega) > 0.$$

After Fourier-Laplace transform and by applying the operator E, we get from (1.1):

$$E\tilde{u} = -2N\left(\frac{\omega}{k}\right) E\left(\frac{\hat{u_1} - i\big(\omega - 2kM(y)\big)\hat{u_0}}{\big(\omega - kM(y)\big)^2}\right), \tag{2.2}$$

where

$$N(\lambda) := \big(2 - F(\lambda)\big)^{-1},$$

with

$$F(\lambda) := \int_{-1}^{1} \frac{1}{\big(\lambda - M(y)\big)^2}\, dy, \qquad \lambda \in \mathbb{C} \setminus [M_-, M_+]. \tag{2.3}$$

One can show that N is meromorphic in $\mathbb{C} \setminus [M_-, M_+]$. We now introduce the following hypothesis:

$(\mathcal{H}_S)$ The function $N(\lambda)$ has no complex (i.e. non real) poles.

This assumption is fundamental. Indeed it is shown in both [2] and [6] that, if N has non real poles, then (1.1) is ill-posed. Moreover, in [2] you can find explicit conditions on M that ensure that $(\mathcal{H}_S)$ is satisfied or not. We now introduce another assumption:

$(\mathcal{H}_{RL})$ $M(y)$ takes the value $M_\pm$ at a point where it has a right or left derivative.

One can see (see again [2]) that, consequently, $N(\lambda)$ has exactly one real pole λ_- (resp. λ_+) in $]-\infty, M_-[$ (resp. in $]M_+, \infty[$).

The next step, the difficult one, is to calculate the inverse Laplace transform of the expression (2.2) of $E\tilde{u}$. This is done, in [6], using integration techniques and contour deformation. Therefore, the poles of N play an important part in the process. Moreover, N has, in general, a cut on Range(M). Hence, N can blow up as we approach the cut from above and below. The calculation was done in [6] for strictly monotonous and convex (or concave), regular profiles. It provides a well-posedness theorem, a quasi-explicit expression and an estimate of the solution. These results are rewritten in Section 2.3.1, where the constant convexity condition is replaced by a less explicit one. In the following section, we give a general theorem based on the same proof.

2.2 A general theorem

For a better understanding we mostly keep the same notation as in [6]. We denote, when it is possible

$$N_{\pm}(\lambda):=\begin{cases} N(\lambda), & \lambda\in\mathbb{C}^{\pm},\\ \lim\limits_{\varepsilon\searrow 0} N(\lambda\pm i\varepsilon), & \lambda\in]M_-,M_+[,\end{cases} \qquad N'_{\pm}(\lambda):=\begin{cases} \dfrac{dN}{d\lambda}(\lambda), & \lambda\in\mathbb{C}^{\pm},\\ \lim\limits_{\varepsilon\searrow 0} \dfrac{dN}{d\lambda}(\lambda\pm i\varepsilon), & \lambda\in]M_-,M_+[,\end{cases}$$

where $\mathbb{C}^{\pm}=\{z\in\mathbb{C}/\pm\mathcal{I}mz>0\}$. Before stating the theorem, we have to introduce two new technical hypotheses:

$(\mathcal{H}_N)$ The function $N_{\pm}$ can be extended by continuity with $N_{\pm}(M_+)=N_{\pm}(M_-)=0$, as a function Hölder continuous in $\mathbb{C}^{\pm}\cup[M_-,M_+]$.

Moreover, $\forall\lambda\in[M_-,M_+]$ we have $N_-(\lambda)=\overline{N_+(\lambda)}$. As a consequence we can write:

$$N_{\pm}(\lambda)=\mathcal{R}N(\lambda)\pm i\mathcal{I}N(\lambda). \tag{2.4}$$

$(\mathcal{H}_{N'})$ The function $N'_{\pm}$ can be extended by continuity to $[M_-,M_+]$ and it satisfies $N'_+(M_\pm)-N'_-(M_\pm)=0$. Then it is Hölder continuous in $\mathbb{C}^{\pm}\cup[M_-,M_+]$.

Moreover, $\forall\lambda\in[M_-,M_+]$ we have $N'_-(\lambda)=\overline{N'_+(\lambda)}$. As a consequence we can write:

$$N'_{\pm}(\lambda)=\mathcal{R}N'(\lambda)\pm i\mathcal{I}N'(\lambda). \tag{2.5}$$

By following the same process as in [6], one can show the following theorem:

Theorem 2.1. *Let us assume that $M\in C^0([-1,1])$ such that $(\mathcal{H}_S)$,$(\mathcal{H}_{RL})$,$(\mathcal{H}_N)$ and $(\mathcal{H}_{N'})$ are satisfied. Then, the Cauchy problem (1.1) is well-posed in the sense that for any $(u_0,u_1)\in L^2_y(H^{3+n}_x)\times L^2_y(H^{2+n}_x)$, $n\geq 0$, where $L^2_y(H^n_x):=L^2(]-1,1[;H^n(\mathbb{R}))$, it admits a unique solution*

$$u\in C^0(\mathbb{R}^+;L^2_y(H^n_x))\cap C^1(\mathbb{R}^+;L^2_y(H^{n-1}_x)).$$

Furthermore we have $Eu(x,t)=-2E[u_p(x,.,t)+u_c(x,.,t)]$ where

- *the poles contribution is:*

$$u_p(x,y,t)=\sum_{\pm}\frac{\int_0^{\lambda_\pm t}u_1(x-s,y)ds}{F'(\lambda_\pm)\left(\lambda_\pm-M(y)\right)}+\sum_{\pm}\frac{\lambda_\pm-2M(y)}{\left(\lambda_\pm-M(y)\right)^2}\frac{u_0(x-\lambda_\pm t,y)}{F'(\lambda_\pm)}, \tag{2.6}$$

- *and the branch cut contribution is:*

$$
\begin{aligned}
&u_c(x,y,t)\\
=&\frac{1}{\pi}\,p.v.\int_{M_-}^{M_+}\frac{\mathcal{I}N(\lambda)}{\lambda-M(y)}\left[u_0(x-\lambda t,y)+tM(y)\frac{\partial u_0}{\partial x}(x-\lambda t,y)+tu_1(x-\lambda t,y)\right]d\lambda\\
&+\frac{1}{\pi}\,p.v.\int_{M_-}^{M_+}\frac{\mathcal{I}N'(\lambda)}{\lambda-M(y)}\left[\int_0^{\lambda t}u_1(x-s,y)\,ds-M(y)u_0(x-\lambda t,y)\right]d\lambda\\
&-\mathcal{R}N\big(M(y)\big)\left[u_0\big(x-M(y)t,y\big)+tM(y)\frac{\partial u_0}{\partial x}\big(x-M(y)t,y\big)+tu_1\big(x-M(y)t,y\big)\right]\\
&-\mathcal{R}N'\big(M(y)\big)\left[\int_0^{M(y)t}u_1(x-s,y)\,ds-M(y)u_0\big(x-M(y)t,y\big)\right],
\end{aligned}
\tag{2.7}
$$

where p.v. stands for the Cauchy principal value integral.

Furthermore we have the following estimate of the mean value:

$$
\|Eu\|_{L^2_x}\le C\left[\|u_0\|_{L^2_y(L^2_x)}+t\left\|\frac{\partial u_0}{\partial x}\right\|_{L^2_y(L^2_x)}+(1+t)\|u_1\|_{L^2_y(L^2_x)}\right]. \tag{2.8}
$$

Finally we get the expression of u from (2.1).

Physical interpretation: This expression gives us a physical interpretation of the solution. Indeed, in the case $u_1=0$, one can check that Eu_p is a solution of the generalized wave equation

$$
\left(\frac{\partial}{\partial t}+\lambda_+\frac{\partial}{\partial x}\right)\left(\frac{\partial}{\partial t}+\lambda_-\frac{\partial}{\partial x}\right)Eu_p=0.
$$

The appearance of such velocities $\lambda_\pm$ in the phenomena is not obvious simply looking at the original model. Furthermore Eu_c is a continuous superposition on λ of squared transport equation:

$$
Eu_c=\int_{M_-}^{M_+}U_{c,\lambda}\,d\lambda,\quad \text{where}\quad \left(\frac{\partial}{\partial t}+\lambda\frac{\partial}{\partial x}\right)^2U_{c,\lambda}=0.
$$

Estimate: The estimate (2.8) predicts a linear growth in time of the norm of the mean value. Using this estimate of the mean value and the fact that u is the solution of a transport squared equation, the authors of [6] get the following estimate

$$
\|u\|_{L^2_y(L^2_x)}\le\|u_0\|_{L^2_y(L^2_x)}+C\sum_{k=1}^{3}t^k\left(\left\|\frac{\partial^k u_0}{\partial x^k}\right\|_{L^2_y(L^2_x)}+\left\|\frac{\partial^{k-1}u_1}{\partial x^{k-1}}\right\|_{L^2_y(L^2_x)}\right),
$$

which predicts a possible polynomial growth in time as t^3. In fact, they did not use that the right-hand side depends on Eu, and consequently on the solution itself. By working on the full expression obtained for u (through (2.1), (2.6) and (2.7)), a linear growth seems more likely. We will confirm it through our simulations.

2.3 Two particular cases

The Theorem 2.1 provides us a quasi explicit expression of the solution. In order to exploit it for numerical simulations we need to get the expressions of $\mathcal{R}N$, $\mathcal{I}N$, $\mathcal{R}N'$, and $\mathcal{I}N'$. This can be done for a class of monotonous profiles, as shown below. After that, we give an example of a non monotonous profile for which it is still possible.

2.3.1 The case of a class of monotonous profiles

We introduce here a class of smooth monotonous profiles:

Definition 2.1. We shall say that a profile M belongs to the class C_s if

- $M\in C^{3,\gamma}([-1,1])$ i.e. M is a real-valued function, 3-times differentiable and its third derivative is Hölder continuous with exponent γ;
- $M'(y)\neq 0$, $\forall\, y\in[-1,1]$;
- $\lim_{\varepsilon\searrow 0} F(\lambda\pm i\varepsilon)-2\neq 0$, $\forall\,\lambda\in\,]M_-,M_+[$.

In what follows, we assume that $M\in C_s$ and, without a loss of generality, that M is increasing. We introduce the inverse function μ of M. Using the change of variable $z=M(y)$ and integration by parts, one can show that for $\lambda\in]M_-,M_+[$ (see, e.g., [8]):

$$\mathcal{R}F(\lambda)=\Big[-\frac{\mu'(z)}{z-\lambda}\Big]_{M_-}^{M_+}+p.v.\int_{M_-}^{M_+}\frac{\mu''(z)}{z-\lambda}\,dz, \tag{2.9a}$$

$$\mathcal{R}F'(\lambda)=\Big[\frac{-\mu'(z)}{(z-\lambda)^2}\Big]_{M_-}^{M_+}-\Big[\frac{\mu''(z)}{z-\lambda}\Big]_{M_-}^{M_+}+p.v.\int_{M_-}^{M_+}\frac{\mu'''(z)}{z-\lambda}\,dz, \tag{2.9b}$$

$$\mathcal{I}F(\lambda)=\pi\mu''(\lambda),\qquad \mathcal{I}F'(\lambda)=\pi\mu'''(\lambda), \tag{2.9c}$$

where

$$\lim_{\varepsilon\searrow 0}F(\lambda\pm i\varepsilon):=\mathcal{R}F(\lambda)\pm i\mathcal{I}F(\lambda),\qquad \lim_{\varepsilon\searrow 0}F'(\lambda\pm i\varepsilon):=\mathcal{R}F'(\lambda)\pm i\mathcal{I}F'(\lambda).$$

Thanks to the third condition of Definition 2.1, the definition of $N_\pm$ and $N'_\pm$ makes sense. Remembering (2.4) and (2.5) we get their expressions, functions of $\mathcal{R}F$, $\mathcal{R}F'$, $\mathcal{I}F$ and $\mathcal{I}F'$:

$$\mathcal{R}N(\lambda)=|N(\lambda)|^2\,(2-\mathcal{R}F(\lambda)),\qquad \mathcal{I}N(\lambda)=|N(\lambda)|^2\mathcal{I}F(\lambda), \tag{2.10a}$$

$$\begin{aligned}\mathcal{R}N'(\lambda)=|N(\lambda)|^4\Big[&\Big(\big(2-\mathcal{R}F(\lambda)\big)^2-\mathcal{I}F(\lambda)^2\Big)\mathcal{R}F'(\lambda)\\ &-2\mathcal{I}F(\lambda)\mathcal{I}F'(\lambda)\big(2-\mathcal{R}F(\lambda)\big)\Big],\end{aligned} \tag{2.10b}$$

$$\begin{aligned}\mathcal{I}N'(\lambda)=|N(\lambda)|^4\Big[&2\mathcal{I}F(\lambda)\big(2-\mathcal{R}F(\lambda)\big)\mathcal{R}F'(\lambda)\\ &+\mathcal{I}F'(\lambda)\Big(\big(2-\mathcal{R}F(\lambda)\big)^2-\mathcal{I}F(\lambda)^2\Big)\Big],\end{aligned} \tag{2.10c}$$

where

$$|N(\lambda)| := \left| \lim_{\varepsilon \searrow 0} N(\lambda \pm i\varepsilon) \right| = \left[(2 - \mathcal{R}F(\lambda))^2 + \mathcal{I}F(\lambda)^2 \right]^{-\frac{1}{2}}.$$

Furthermore it is shown in [6] that for such a profile, $(\mathcal{H}_N)$ and $(\mathcal{H}_{N'})$ are satisfied. $(\mathcal{H}_{RL})$ is obviously satisfied. We now get the following theorem as a direct consequence of Theorem 2.1:

Theorem 2.2. *Let us assume that $M \in C_s$ and that $(\mathcal{H}_S)$ is satisfied. Then, the Cauchy problem* (1.1) *is well-posed in the sense that for any $(u_0, u_1) \in L^2_y(H^{3+n}_x) \times L^2_y(H^{2+n}_x)$, $n \geq 0$, it admits a unique solution*

$$u \in C^0(\mathbb{R}^+; L^2_y(H^n_x)) \cap C^1(\mathbb{R}^+; L^2_y(H^{n-1}_x)).$$

Furthermore we have $Eu(x,t) = -2E[u_p(x,.,t) + u_c(x,.,t)]$ where u_p is given by (2.6) *and u_c by* (2.7) *and* (2.10)*. Moreover the estimates* (2.8) *still hold. Finally we get u from* (2.1)*.*

Remark 2.1. If we replace, in Definition 2.1, the third condition by $M''(y) \neq 0$, $\forall y \in [-1,1]$, then (2.9) implies $\lim_{\varepsilon \searrow 0} F(\lambda \pm i\varepsilon) - 2 \neq 0$ for all $\lambda \in]M_-, M_+[$ (since its imaginary part is non zero). Moreover, it is shown in [6] that $(\mathcal{H}_S)$ is automatically satisfied. Then we get the well-posedness theorem written in [6].

This theorem provides us a quasi-explicit expression of the solution for a large class of profiles. We are going to use this expression for numerical simulations (see Section 3.2). However, non-monotonous profiles do not belong to this class. That is why we have given Theorem 2.1 which can be used case by case, for more general profiles as it is shown in the following section.

2.3.2 The case of a non monotonous profile: $M(y) = 1 - y^2$

This section is devoted to the study of a non monotonous profile. To apply Theorem 2.1 the difficulty is to calculate $\lim_{\varepsilon \searrow 0} N(\lambda \pm i\varepsilon)$. In opposition to a C_s profile, no general method can be used. This section can be seen as a procedure to follow for more general profiles. We consider here a quadratic profile:

$$M(y) = 1 - y^2.$$

It was chosen because its behaviour is well fitted to the physics of a reference flow in a duct. In order to apply Theorem 2.1, we have to show that we are in its framework of application. First of all $(\mathcal{H}_{RL})$ is obviously satisfied. From the concavity of M we get that $(\mathcal{H}_S)$ is satisfied too (see [2]). We now want to show that $(\mathcal{H}_N)$ and $(\mathcal{H}_{N'})$ are satisfied.

In what follows we take the branch cut of the complex square root and of the complex logarithm function along the real axis.

Calculation of $\mathcal{R}N$ and $\mathcal{I}N$: We begin with the calculation of $\lim_{\varepsilon\searrow 0} F(\lambda\pm i\varepsilon) := \mathcal{R}F(\lambda) \pm i\mathcal{I}F(\lambda)$, for $\lambda\in]0,1[$ (note that here $M_-=0$ and $M_+=1$). In this purpose, we are going to calculate

$$F(\lambda)=\int_{-1}^{1}\frac{1}{(\lambda-1+y^2)^2}\,dy$$

for λ such that $\mathcal{I}m(\lambda)\neq 0$. We use the following partial fraction expansion

$$\begin{aligned}\frac{1}{(\lambda-1+y^2)^2}=&\frac{1}{4(1-\lambda)}\left[\frac{1}{(y-\sqrt{1-\lambda})^2}+\frac{1}{(y+\sqrt{1-\lambda})^2}\right]\\&+\frac{1}{4(1-\lambda)\sqrt{1-\lambda}}\left[\frac{1}{y+\sqrt{1-\lambda}}-\frac{1}{y+\sqrt{1+\lambda}}\right]\end{aligned}$$

to obtain

$$\begin{aligned}F(\lambda)=&\frac{-1}{(1-\lambda)\lambda}+\frac{1}{4(1-\lambda)\sqrt{1-\lambda}}\left[\log\left(1+\sqrt{1-\lambda}\right)\right.\\&\left.-\log\left(1-\sqrt{1-\lambda}\right)+\log\left(-1-\sqrt{1-\lambda}\right)-\log\left(-1+\sqrt{1-\lambda}\right)\right].\end{aligned}$$

One can easily get, for any $\lambda\in]0,1[$:

$$\mathcal{R}F(\lambda)=\frac{-1}{(1-\lambda)\lambda}+\frac{1}{2(1-\lambda)\sqrt{1-\lambda}}\log\left(\frac{1+\sqrt{1-\lambda}}{1-\sqrt{1-\lambda}}\right),\tag{2.11a}$$

$$\mathcal{I}F(\lambda)=\frac{\pi}{2(1-\lambda)\sqrt{1-\lambda}}.\tag{2.11b}$$

Since $\mathcal{I}F(\lambda)\neq 0$, we have $\lim_{\varepsilon\searrow 0}F(\lambda\pm i\varepsilon)\neq 2$ and we get the expression of $\mathcal{R}N$ and $\mathcal{I}N$ from (2.10).

Calculation of $\mathcal{R}N'$ and $\mathcal{I}N'$: By a similar process we get:

$$\mathcal{R}F'(\lambda)=\frac{-2+5\lambda}{2(1-\lambda)^2\lambda^2}-\frac{3}{4(1-\lambda)^2\sqrt{1-\lambda}}\log\left(\frac{1+\sqrt{1-\lambda}}{1-\sqrt{1-\lambda}}\right),\tag{2.12a}$$

$$\mathcal{I}F'(\lambda)=-\frac{3\pi}{4(1-\lambda)^2\sqrt{1-\lambda}}.\tag{2.12b}$$

Once again we get the expression of $\mathcal{R}N'$ and $\mathcal{I}N'$ from (2.10).

Using the results above one can show that $(\mathcal{H}_N)$ and $(\mathcal{H}'_N)$ are satisfied. Finally, we can apply Theorem 2.1 to get a quasi-analytic expression of Eu and then of u. The results of the numerical computation of the solution are presented in Section 3.2.2.

3 Numerical computation of the solution

In this section, we present the numerical method and we illustrate it by three examples, the linear and tangent profiles, which belong to the C_s class, and the quadratic profile $M(y)=1-y^2$.

3.1 The numerical method

We assume here that M is such that we can apply Theorem 2.1, and that we have obtained the expressions of the functions $\mathcal{R}N$, $\mathcal{I}N$, $\mathcal{R}N'$, $\mathcal{I}N'$. In the case of a C_s profile these expressions are given by (2.10) through (2.9). In the case of $M(y)=1-y^2$ they are given by (2.10) through (2.11) and (2.12).

Thanks to Theorem 2.1, we get a quasi-explicit expression of $Eu=E[u_p+u_c]$ (through multiple integrals) through (2.6) and (2.7). We are now going to explain how we proceed to compute numerically the solution. Our main tool will be the Gauss-Legendre quadrature, to compute integrals. For more details, see [9].

Numerical computation of Eu: First of all, to avoid the computation of terms of the form $\int_0^{\mu t} u_1(x-s,y)\,ds$ we assume that we know a primitive of u_1. Moreover we assume that we have analytic expressions of the initial conditions and the profile (and its inverse). One can easily free himself from these technical assumptions. This is now how we proceed:

1. We initialize the functions, F, F', $\mathcal{R}N$, $\mathcal{R}N'$, $\mathcal{I}N$ and $\mathcal{I}N'$, using a gaussian quadrature to compute the integrals. We use at most 64 quadrature points. When it is necessary (as in the case of a C_s profile, see (2.9)), we use the following definition of the Cauchy principal value integral (see [8]):

$$v.p.\int_{M_-}^{M_+}\frac{\phi(\lambda)}{\lambda-x}\,d\lambda=\int_{M_-}^{M_+}\frac{\varphi(\lambda)-\varphi(x)}{\lambda-x}\,d\lambda+\varphi(x)\log\left(\frac{M_+-x}{x-M_-}\right). \tag{3.1}$$

2. Since F is monotonous in $]M_+,\infty[$ (resp. $]-\infty,M_-[$) we get λ_+ (resp. λ_-) by dichotomy. From (2.6) we get u_p.
3. To compute u_c, we use the definition (3.1) of the Cauchy principal value integral.
4. Finally, we get $Eu=E[u_p+u_c]$ by integrating with respect to y, using again, a Gaussian quadrature.

Numerical computation of u: Derivating the expression of Eu two times with respect to x, only consists in derivating two times the initial conditions. We obtain an expression for $\partial^2 Eu/\partial x^2$ that we compute using the same process as we did for Eu. Finally we get u by (2.1).

Remark 3.1. We only need the values of the functions $\mathcal{R}N$, $\mathcal{I}N$, $\mathcal{R}N'$, and $\mathcal{I}N'$ at the quadrature points. Therefore, we compute them, once and for all, at the beginning of our program.

Remark 3.2. The precision of this computation is, unfortunately, dependent on the time t. Indeed, the integration interval grows with t in the expression (2.1) of u. Moreover, the functions we integrate, such that $tu_1(x-\lambda t,y)$ in (2.7), get worse and worse with time (in the sense that they become more difficult to integrate). The solution consists in increasing the number of quadrature points.

3.2 Numerical computation for smooth monotonous profiles

In this section, for both linear and tangent profiles, we first show that they belong to the C_s class and then we give the numerical results obtained.

3.2.1 The linear profile

We now consider the particular case of a linear profile $M(y)=My$ where $M\in\mathbb{R}_+^*$. We are going to see how to use Theorem 2.2. In that case F can be explicitly calculated. Indeed, a simple integration gives for $\lambda\in\mathbb{C}\setminus[-M,M]$:

$$F(\lambda)=\frac{2}{\lambda^2-M^2}.$$

As a consequence, the solutions of $F(\lambda)=2$ for $\lambda\in\mathbb{C}\setminus[-M,M]$ are $\lambda_\pm=\pm\sqrt{1+M^2}$, so that $(\mathcal{H}_S)$ is satisfied. From (2.9) and (2.10) or directly, one can easily get for $\lambda\in]-M,M[$:

$$\mathcal{R}F(\lambda)=\frac{2}{\lambda^2-M^2},\qquad \mathcal{I}F(\lambda)=0, \tag{3.2a}$$

$$\mathcal{R}F'(\lambda)=\frac{-4\lambda}{(\lambda^2-M^2)^2},\qquad \mathcal{I}F'(\lambda)=0, \tag{3.2b}$$

$$\mathcal{R}N(\lambda)=\frac{1}{2-\mathcal{R}F(\lambda)},\qquad \mathcal{I}N(\lambda)=0, \tag{3.2c}$$

$$\mathcal{R}N'(\lambda)=\frac{\mathcal{R}F'(\lambda)}{(2-\mathcal{R}F(\lambda))^2},\qquad \mathcal{I}N'(\lambda)=0. \tag{3.2d}$$

In particular, since $\mathcal{R}F(\lambda)\neq 2$, the third condition of Definition 2.1 is fulfilled and $M\in C_s$.

Numerical results: We present here the solution for $M=1$. We have taken $u_0(x,y)=e^{-x^2}$, a gaussian function with respect to x, independent of y and $u_1(x,y)=0$. We begin with the time evolution of the mean value Eu, where x varies from -15 to 15 on the abscissa, see Fig. 1. The red arrows move at velocities $\lambda_\pm$; they point out the contribution of the poles. By this way, we can separate the two contributions, the rest representing the contribution

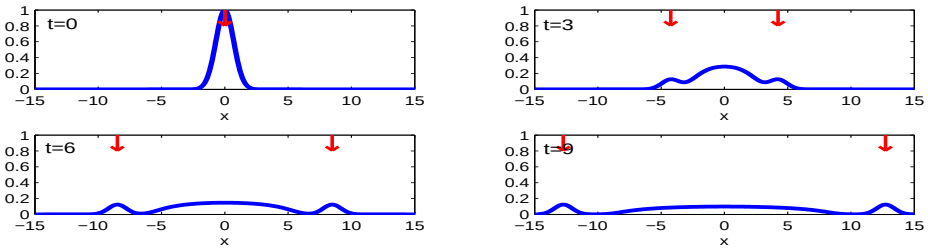

Figure 1: Time evolution of Eu for $M=1$.

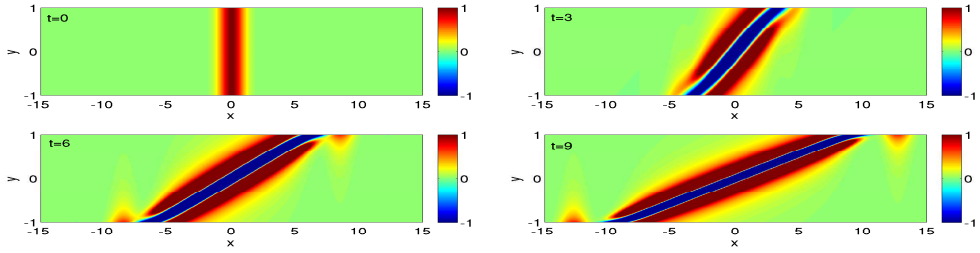

Figure 2: Time evolution of u for $M=1$.

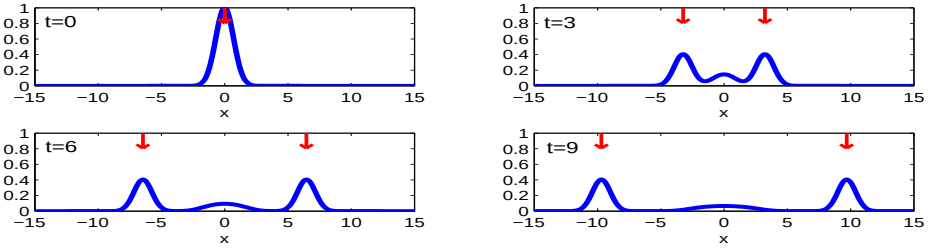

Figure 3: Time evolution of Eu for $M=0.4$.

of the branch cut. As the poles velocities are greater than the branch cut velocities ($\in [M_-,M_+]$, see Section 2.2), the distinction between the two contributions is easier when time increases. We notice that the amplitude of the poles contribution decreases until a limit value while the branch cut's is widening and decreasing. We now present the time evolution of u, where x is on the abscissa and y on the ordinate, see Fig. 2.

We now see the phenomena for each y; in opposition to Eu, u is no more symmetric with respect to x. We notice again the distinction between the two contributions. The branch cut contribution is the most visible one and represents the convection. Indeed, this contribution takes on the behaviour of the profile (it is verified in all the examples presented hereinafter). The contribution of the poles is smaller and localized at the boundary $y=\pm 1$. More precisely, the contribution of the pole λ_+ (resp. λ_-) is localized in $y=1$ (resp. $y=-1$), where the profile takes its maximum (resp. minimum) value. We now present

the evolution of the mean value for $M=0.4$ in Fig. 3.

We notice that the poles contribution is more important than in the previous case. What is remarkable is that when M tends to 0 this contribution becomes predominant and the mean value tends to the solution of a wave equation. Indeed, in the simple case of the uniform flow ($M(y)=M$), taking the mean value of the equation shows that $\psi=Eu$ is a solution of the convected wave equation

$$\left(\frac{\partial}{\partial t}+M\frac{\partial}{\partial x}\right)^2\psi-\frac{\partial^2\psi}{\partial x^2}=0.$$

3.2.2 The tangent profile

We consider here a tangent profile:

$$M(y)=\tan\left(\frac{\pi}{2}-\alpha\right)^{-1}\tan\left(\left(\frac{\pi}{2}-\alpha\right)y\right),$$

where $\alpha\in]0,\pi/2[$ and $\tan(\pi/2-\alpha)^{-1}$ is a normalization factor. In particular we have $M_-=-1$ and $M_+=1$. This profile is increasing, concave on $]-1,0[$ and convex on $]0,1[$. We know from [2] that for such a profile, $(\mathcal{H}_S)$ is satisfied. To show that $M\in C_s$, the only difficulty is to show the third condition of Definition 2.1. From (2.9) (which hold as soon as $M\in C^2([-1,1])$ and $M'(y)\neq 0, \forall y\in[-1,1]$) we get that $\mathcal{I}F(\lambda)$ vanishes only for $\lambda=0$. Hence, to conclude we only have to verify that $\mathcal{R}F(0)\neq 2$, what is done numerically.

We now present the results obtained for $u_1(x,y)=0$ and $u_0(x,y)=e^{-x^2}$. Fig. 4 represents the time evolution of the mean value for $t=0,3,6$ and 9, and Fig. 5 represents the time evolution of function u itself at the same time. The red arrows move at velocities $\lambda_-\approx-1.21096$ and $\lambda_+\approx 1.21096$. Here again we can see the two contributions. The same remarks as in the linear case still hold.

3.3 The quadratic profile $M(y)=1-y^2$

Numerically we get $\lambda_-\approx-0.4909$ and $\lambda_+\approx 1.7683$. We take again $u_1(x,y)=0$ and $u_0(x,y)=e^{-x^2}$. Fig. 6 represents the evolution of the mean value and Fig. 7 represents u at the same time, for $x\in[-8,24]$. Once again the red arrows move at velocities $\lambda_\pm$. We can see on both Figs. 6 and 7 that the amplitude of the contribution of λ_+ (which propagates upstream) is smaller than that of λ_- (which propagates downstream). Once again, the contribution of λ_+ is localized where M takes its maximum (at $y=0$) and the contribution of λ_- is localized where M takes its minimum (at $y=\pm 1$). Furthermore, the fact that $|M_+|>|M_-|$ coincides with the fact the contribution of λ_+ is smaller than λ_-'s.

3.4 Time dependence of the norm of the solution

It is noticed that in the previous examples that we do not see a growth (see Section 2.2), neither for Eu nor for u. This comes from the choice of the initial conditions. To see

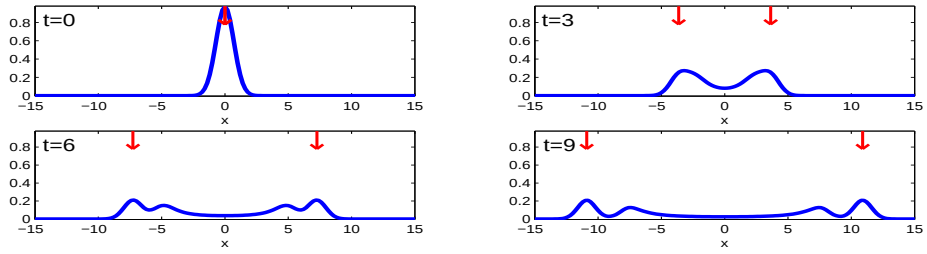

Figure 4: Time evolution of Eu.

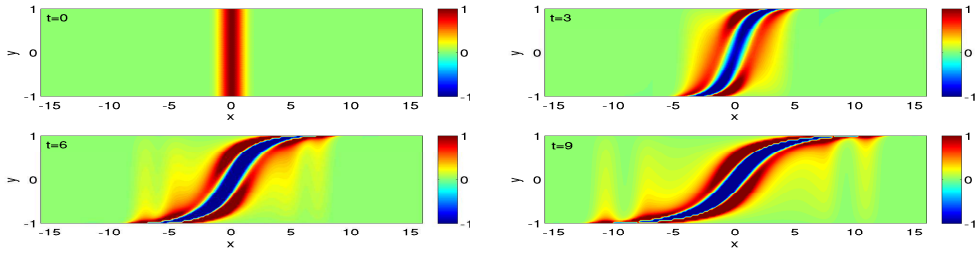

Figure 5: Time evolution of u.

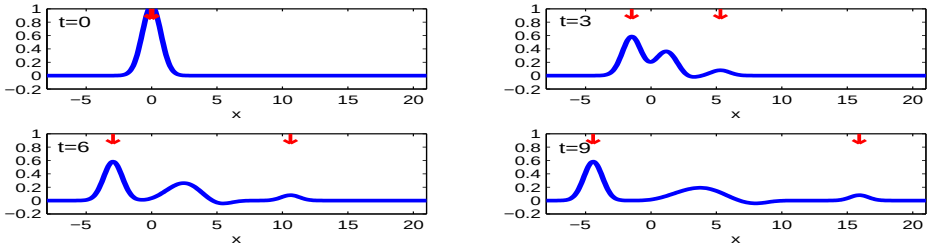

Figure 6: Time evolution of Eu.

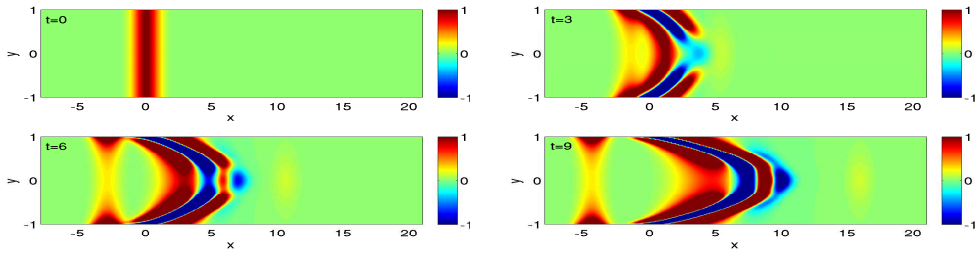

Figure 7: Time evolution of u.

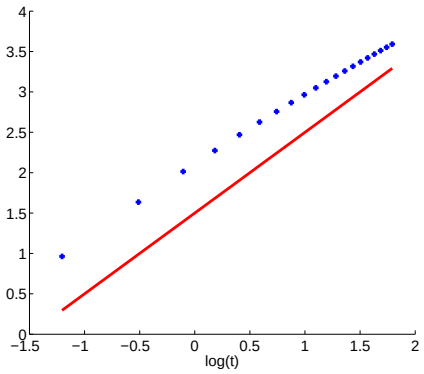

Figure 8: Eu norm.

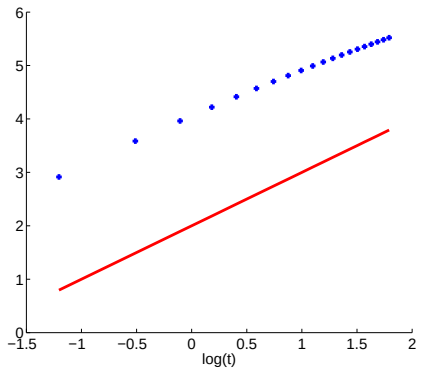

Figure 9: u norm.

a growth of the solution, expressions (2.6) and (2.7) suggest to take for example u_1 (or $\partial u_0/\partial_x$) in $L^2_x(\mathbb{R})$ but not in $L^1_x(\mathbb{R})$. We build such a function f:

$$f(x)=\begin{cases} 2-14x^4+28x^5-20x^6+5x^7, & |x|<1,\\ \dfrac{1}{|x|}, & |x|\geq 1. \end{cases}$$

In particular, $f\in C^4(\mathbb{R})$. In fact, f was built in this purpose.

We now present the evolution of the L^2 norm of Eu and u for the tangent profile with $\alpha=0.2$. The initial conditions are $u_0(x,y)=0$ and $u_1(x,y)=f(x)$. Fig. 8 (resp. Fig. 9) represents, in blue crosses, the evolution of $\log(\|Eu\|_{L^2_x})$ (resp. $\log(\|u\|_{L^2_x(L^2_y)})$) with respect to $\log(t)$. The red lines are reference lines with slopes equal to 1. As a conclusion we see that the growth in time of the solution and its mean value is linear. In all our simulations we have never observed a greater growth.

4 Numerical validation of the model

To validate our asymptotic model (1.1) we are going to compare, numerically, our solution to the solution of the linearized Euler equations in a duct: $(x,Y)\in\mathbb{R}\times[-\varepsilon,\varepsilon]$. Using the equivalence between Galbrun's equations and linearized Euler equations (see [7]) and remembering the scale used to derivate (1.1), we need the solution of the following linearized Euler equations: for $(x,Y)\in\mathbb{R}\times[-\varepsilon,\varepsilon]$, $t\in\mathbb{R}^+$,

$$\begin{cases} \dfrac{\partial U_\varepsilon}{\partial t}+M\left(\dfrac{Y}{\varepsilon}\right)\dfrac{\partial U_\varepsilon}{\partial x}+\dfrac{\partial P_\varepsilon}{\partial x}+\dfrac{1}{\varepsilon}M'\left(\dfrac{Y}{\varepsilon}\right)V_\varepsilon=0,\\ \dfrac{\partial V_\varepsilon}{\partial t}+M\left(\dfrac{Y}{\varepsilon}\right)\dfrac{\partial V_\varepsilon}{\partial x}+\dfrac{\partial P_\varepsilon}{\partial Y}=0,\\ \dfrac{\partial P_\varepsilon}{\partial t}+M\left(\dfrac{Y}{\varepsilon}\right)\dfrac{\partial P_\varepsilon}{\partial x}+\dfrac{\partial U_\varepsilon}{\partial x}+\dfrac{\partial V_\varepsilon}{\partial Y}=0, \end{cases} \tag{4.1}$$

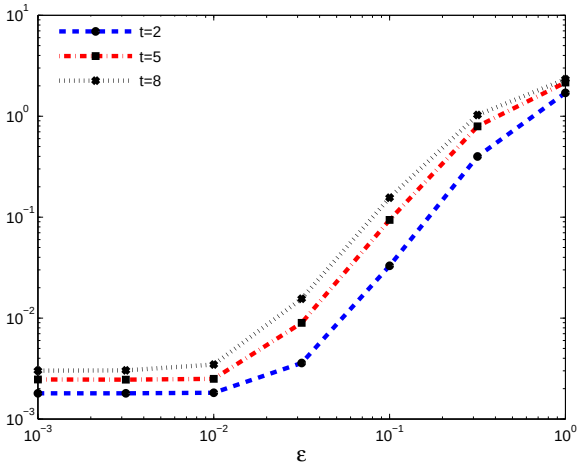

Figure 10: The relative error for $t=2$, 5 and 8 in a logarithmic scale.

where $(U_\varepsilon, V_\varepsilon)$ are the two components of the Eulerian velocity and P_ε is the pressure. Furthermore we obtain the following initial conditions for $(x,Y)\in\mathbb{R}\times[-\varepsilon,\varepsilon]$, functions of (u_0,u_1) the initial condition of (1.1):

$$U_\varepsilon(x,Y,0)=u_1\left(x,\frac{Y}{\varepsilon}\right)+M\left(\frac{Y}{\varepsilon}\right)\frac{\partial u_0}{\partial x}\left(x,\frac{Y}{\varepsilon}\right),$$
$$V_\varepsilon(x,Y,0)=0,\quad P_\varepsilon(x,Y,0)=-\frac{\partial u_0}{\partial x}\left(x,\frac{Y}{\varepsilon}\right).$$

Marc Duruflé, using its Montjoie code[†], solved (4.1) using discontinuous Galerkin spectral method (for more precision see [4]). He provided us P_ε for several ε.

To compare the results we have to express u, the solution of (1.1), into Eulerian variables. Using again the equivalence between Galbrun's equations and linearized Euler equations and the asymptotic expansions used in [2] we denote:

$$p(x,y,t):=-\frac{\partial Eu}{\partial x}(x,t),\qquad (x,y)\in\mathbb{R}\times[-1,1],\qquad t\in\mathbb{R}^+,$$

where p is the pressure like function corresponding to our asymptotic model. As a consequence it should be the limit of $p_\varepsilon(x,y,t):=P_\varepsilon(x,\varepsilon y,t)$ when ε tends to 0. We notice that p is independent of y.

We consider the linear case $M(y)=y$ with the following initial conditions: $u_0(x,y)=\exp(-x^2)$ and $u_1(x,y)=0$. We get u, and then p, using the numerical method presented in the previous section. Fig. 10 represents, in a logarithmic scale, the relative error

$$\frac{\|p-p_\varepsilon\|_{L^2(\mathbb{R}\times]-1,1[)}}{\|p\|_{L^2(\mathbb{R}\times]-1,1[)}}$$

[†]https://gforge.inria.fr/projects/montjoie

with respect to ε. We can see that the relative error tends to 0 as ε tends to 0 which validates our asymptotic model. Actually it does not tend to 0 but to a small value (which is between 10^{-2} and 10^{-3} for each t). This is the consequence of the approximation errors of both numerical methods. As these approximation errors increase with t, it explains also why the relative error increases with respect to t. Finally, we observe that the relative error has a quadratic dependance on ε, that is to say that it decreases as ε^2. This remains to be proven.

Acknowledgments

The authors would like to thank Marc Duruflé for his time, effort and kindness.

References

[1] A.S. Bonnet-BenDhia, M. Duruflé, and P. Joly. Construction et analyse mathématique d'un modèle approché pour la propagation d'ondes acoustiques dans un tuyau mince parcouru par un fluide en écoulement. Technical report, INRIA Research Report, 2007.
[2] A.S. Bonnet-BenDhia, M. Duruflé, P. Joly, and L. Joubert. Stability of acoustic propagation in a 2d flow duct: A low frequency approach. submitted.
[3] E.J. Brambley. Fundamental problems with the model of uniform flow over acoustic linings. Journal of Sound and Vibration, 322(4-5):1026–1037, 2009.
[4] N. Castel, G. Cohen, and M. Duruflé. Application of Discontinuous Galerkin spectral method on hexahedral elements for aeroacoustic. Journal of Computational Acoustics, 17(2):175–196, 2009.
[5] H. Galbrun. Propagation d'une onde sonore dans l'atmosphère terrestre et théorie des zones de silence. Gauthier-Villars, Paris, 1931.
[6] P. Joly and R. Weder. A quasi 1D model for aeroacoustics in thin ducts. Submitted.
[7] G. Legendre. Rayonnement acoustique dans un fluide en écoulement: Analyse mathématique et numérique de l'équation de Galbrun. PhD thesis, 2003.
[8] L. Schwartz. Theorie des Distributions. Hermann, Paris, 1950.
[9] A.H. Stroud and D. Secrest. Gaussian Quadrature Formulas. Prentice-Hall Englewood Cliffs, NJ, 1966.